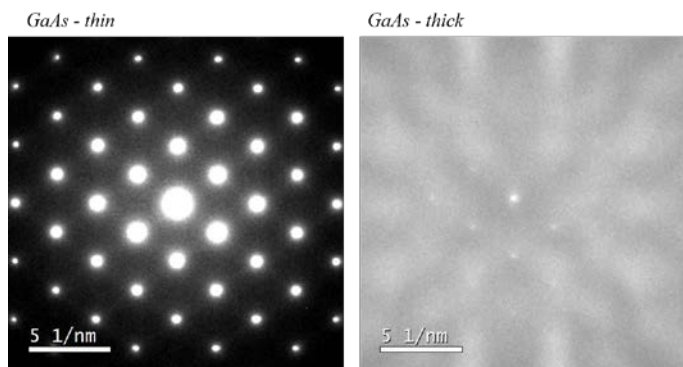


Chapter 20: Convergent-beam diffraction

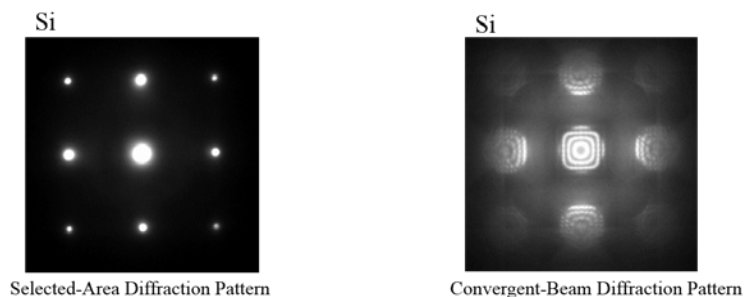
Selected-area diffraction: Influence of thickness

Selected-area diffraction patterns don't generally get much better when the specimen gets thicker. Sometimes a faint feature will be enhanced a bit that we may want to see, but mostly we just get more diffuse scattering and Kikuchi bands that are not especially revealing about the crystal structure.



Selected-area vs. convergent-beam diffraction

Convergent-beam diffraction is another useful mode of diffraction. Instead of sharp spots, CBED patterns give diffraction disks that may contain complicated intensity features. Each mode has some advantages.



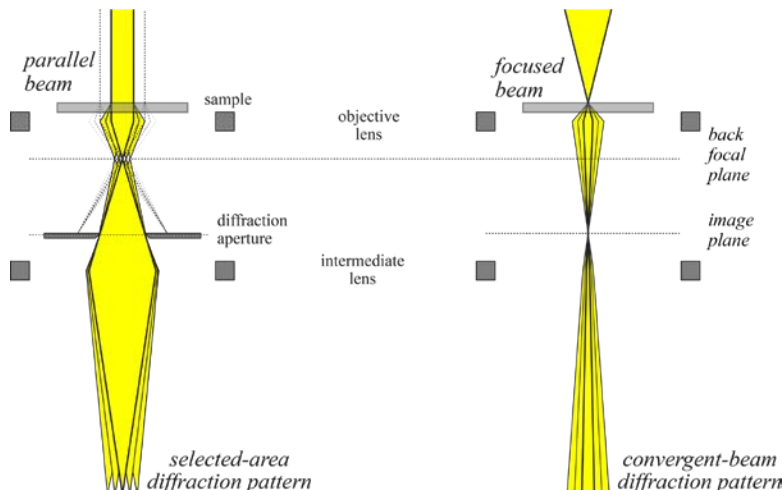
Selected-area diffraction patterns are easy to index, because the spots are nearly point-like. The sharp spots make it easy to measure d-spacing, since we can locate their centers precisely. And we can isolate low-angle features, such as superlattice diffraction satellites without too much trouble, because there is not much overlap among closely spaced diffraction features.

Convergent-beam diffraction patterns generally contain more crystallographic, especially 3-D, information (though it may be challenging to extract some of that information.) CBED samples specific, nanoscale-sized areas, so we can acquire patterns from particular small features of interest. Also, since any tiny area is - in a sense - more uniform than a larger area, Kikuchi lines are usually sharper in CBED.

Ray diagrams for SA and CB diffraction

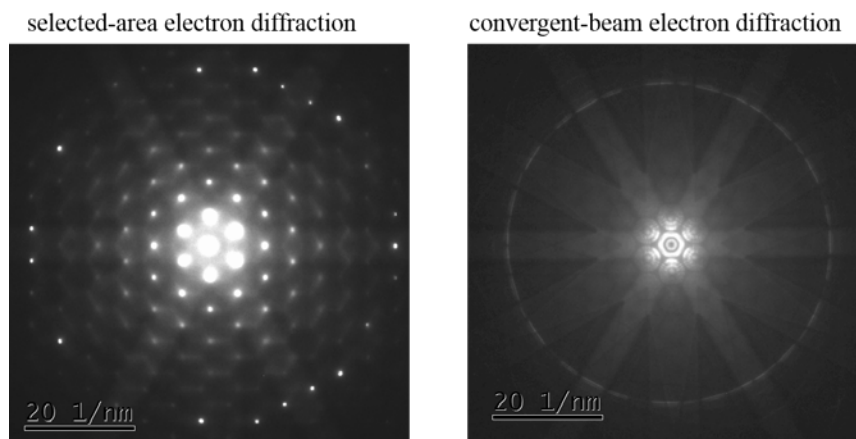
Changing from selected-area to convergent-beam diffraction is very easy. The optics after the sample should be identical, except that we don't need the selected-area diffraction aperture. Above the sample, though, we want to converge the beam to a crossover on the sample, using the condenser lens, of course. Usually, this is done in imaging mode so we can make sure the probe is small and focused. It is sometimes necessary to correct the condenser stigmatism here, if the beam spot does not look very circular. I wouldn't recommend doing this on the CCD camera, because the intensity of the spot is very high. (It's about the same as the direct beam in diffraction mode using parallel illumination with no selected-area

aperture in.) Then, as usual, we switch to diffraction mode, which causes the intermediate lens to focus on the BFP of the objective lens. From the ray diagram, it is less obvious that the BFP represents the diffraction pattern in this case, but we the camera length has been calibrated for these settings, so we especially do not want to change the objective lens focus at this point. The IL can be focused a bit, but it is even tricky to know exactly when a CBED pattern is focused.



Example: Si<111>

Compare a selected-area pattern and a CBED pattern acquire from the same sample under nominally identical conditions. We see stronger Kikuchi lines, because the variations in crystal orientation that might smear them out in selected-area diffraction are much smaller in the small volume sampled by the convergent probe. The HOLZ rings are sharper, too, and almost continuous around their circumference. This is because the ring is strongest in CBED wherever a HOLZ reflection reaches the Bragg condition, not where the relrod crosses the Ewald sphere. Another result is that the diameter of the HOLZ ring is more well-defined for measurement.

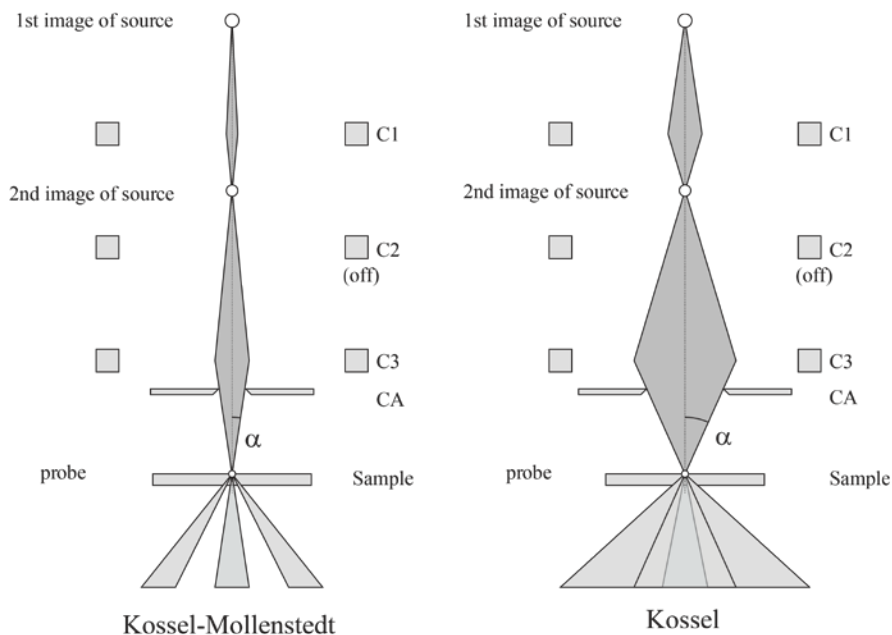


The features within the CBED disks have information, too, that we will analyze shortly.

Influence of convergence angle

The diameter of the CBED disks corresponds to the convergence angle α of the incident probe. We saw that the most immediate influence on α is the condenser aperture diameter, though it can also be controlled using the condenser lens settings. The separation of the disks depends on the crystal structure,

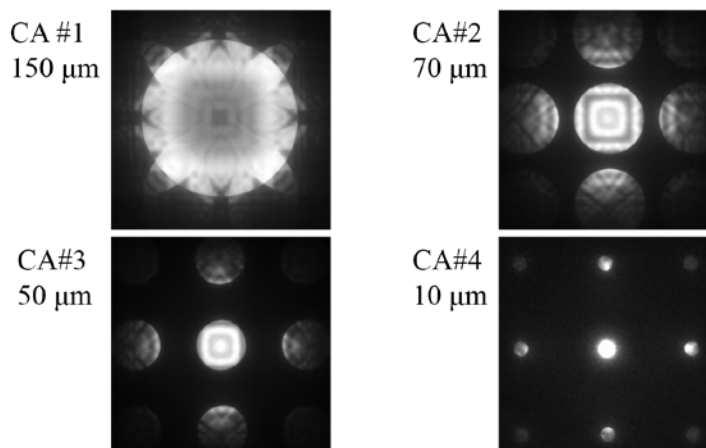
so that shouldn't change if we change α . Normally, we don't want the disks to overlap (though we probably want their diameters to be as large as possible). If the disks don't overlap, the pattern is called a Kossel-Mollenstedt (K-M) pattern.



For larger α , the disks will overlap, producing a Kossel (K) pattern. If the electron source is highly coherent, there can be interesting information about the relative phases of the structure factors in the overlap region. Unfortunately, the amount of coherence has to be very high, or else the crystal's unit cell very large, to see these effects. So with a thermionic electron source, we usually acquire CBED patterns with a K-M condition, instead.

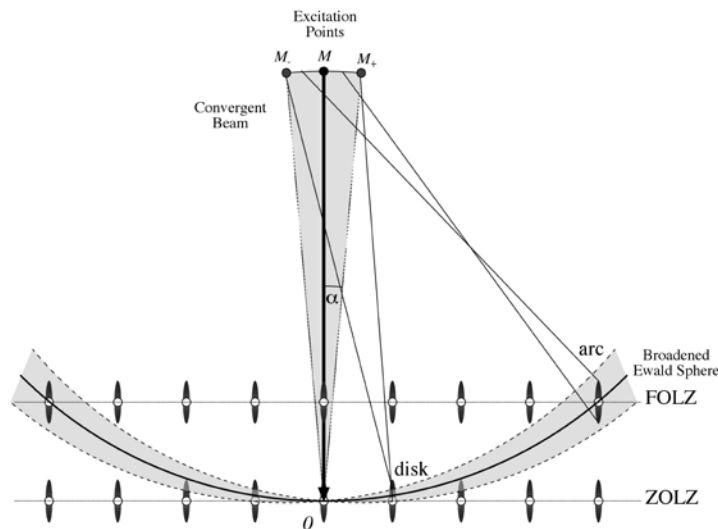
Influence of condenser aperture size

The outer edge of the CBED disks is defined by the CA, so it directly affects the disk diameter. (In principle, they all have the same diameter in a single pattern.) We know the CA doesn't affect the camera length, and changing to a smaller-sized CA doesn't change the intensity variations with each disk, except to define where its hard edge appears. Now, if we orient on a zone axis, we might notice that the outer edges of the higher-angle reflections are not so sharply defined, because the excitation of the spot gets weaker moving outward.



CBED disks and HOLZ rings

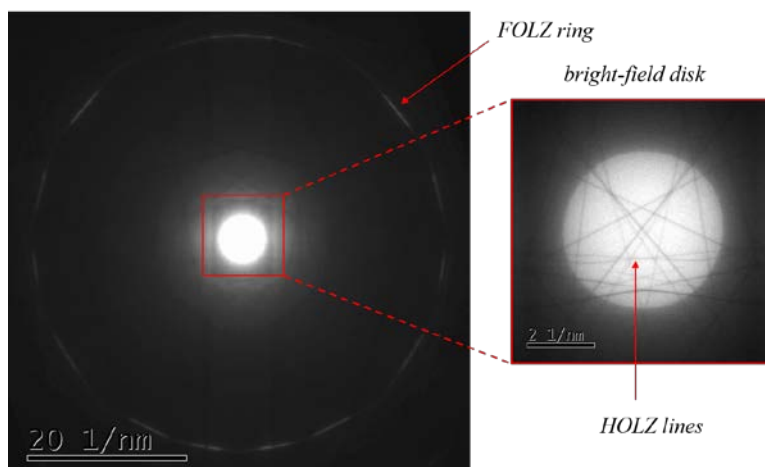
In CBED, we can't even think about our reliable, old Ewald sphere in the same way. Because there is a range of incident beam directions, there is a range of excitation points, with an Ewald sphere essentially center around each of these points. The excitation points trace out a spherical section in reciprocal space. The crystal and its reldods are still the same.



CBED features (I)

The features in a CBED patterns depend on where we look and the camera length we use. On low-index zone axes, we see roughly sinusoidal intensity variations, particularly in the 0 and low-angle g beams. These are called K-M fringes. They are really the pendellosung oscillations we discussed before, due to the range of orientations of the beam with respect to the crystal and changes in excitation for each incident direction.

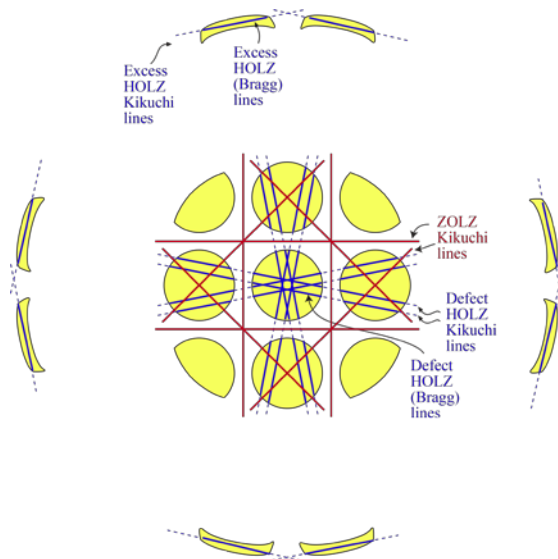
Higher-index patterns tend to show more HOLZ rings that can be found at short camera length. At longer camera length, the features in the 0 disk, which is called the “bright-field” disk, are called HOLZ lines.



CBED features (II)

HOLZ lines that appear in the BF disk on high-index (lower symmetry) zone axes are very sharp, linear features. If the sample is thick enough, we can see how these connect to HOLZ Kikuchi lines that continue outside of the disks. The HOLZ lines within the disk should really be called “defect HOLZ

Bragg lines". They result from Bragg diffraction into a segment of a HOLZ ring at some higher angle, leaving a dark, shadow-like trace showing the where the diffracted electrons came from. Though they are related to the Kikuchi lines, they are the results of just the usual coherent Bragg diffraction, not incoherent, Kikuchi diffraction. The fact that the lines can be very sharp and intersect in an intricate pattern makes them very useful for precision measurements. The trajectories of the HOLZ lines are very sensitive to slight changes in lattice parameter.



CBED bright-field patterns

The intensity within the 0, or BF disk, is called the “bright-field” CBED pattern. We can find the equation for a HOLZ line within the BF disk fairly easily. It occurs where the Bragg condition for some HOLZ reflection \mathbf{g} is satisfied, so for that reflection, the incident beam wave vector has

$$k = |\mathbf{k} + \mathbf{g}|$$

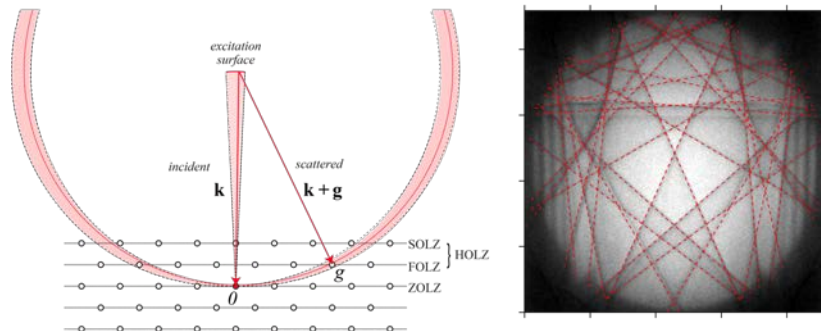
If we square this, we get the equation

$$0 = g_x \cdot k_x + g_y \cdot k_y + g_z \cdot k_z + \frac{g^2}{2}$$

In the BF disk, the tilt of our incident beam must be less than α , which is usually very small (tens of mrad, at most). So we can approximate $k_z \approx -k$. Then we have an equation for a line in the x-y plane with coordinates (k_x, k_y)

$$g_x \cdot k_x + g_y \cdot k_y = -g_z \cdot k - \frac{g^2}{2}$$

By determining the equation for the line, we can find \mathbf{g} and/or k , allowing refinement of the crystal structure or beam energy, respectively.

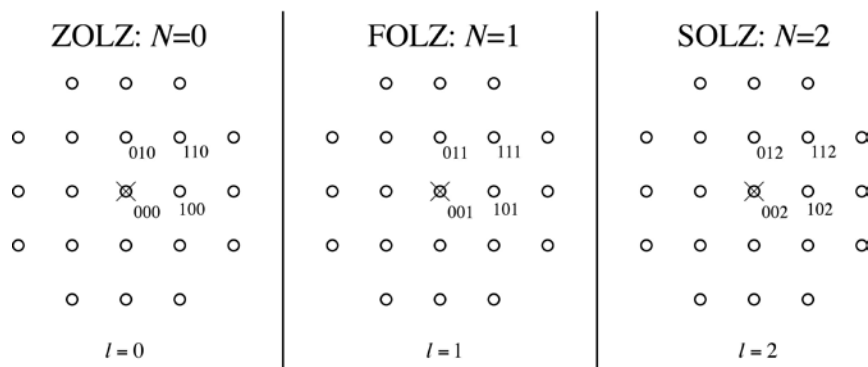


ZAP indexing example: sc [001]

We looked at indexing ZOLZ patterns. We will refer to the diagram of a diffraction pattern from Laue zone of any order as a zone-axis pattern (ZAP). The Miller indices hkl for the reflections on any $[uvw]$ ZAP satisfy the Weiss zone law:

$$hu + kv + \ell w = N$$

where N is an integer. (It is usually non-negative, in practice, because only the Laue zones with $N \geq 0$ intersect the Ewald sphere.)



The first example is a series of ZAPs from a sc crystal in [001] orientation. The zone law for any of these zones is simply $\ell = N$.

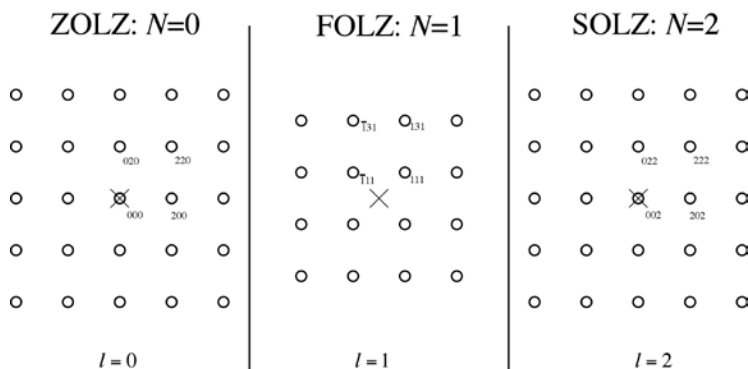
We know there are no restrictions on the hkl for allowed reflections from an sc crystal. The ZOLZ always contains the direct beam 000. So the ZOLZ must have $N = 0$. So the zone law for this ZOLZ is $\ell = 0$. Also in this zone are 100, 010, and 110, and every combination of the form $hk0$.

Next consider $N = 1$. I usually put an \times to locate the projected position of θ in each ZAP. Are there any allowed reflections in this zone, i.e. $\ell = 1$? If we can find even one, then $N = 1$ is the FOLZ. Yes, there are some reflections. In fact every combination of the form $hk1$ is in this zone, e.g., 011, 111.

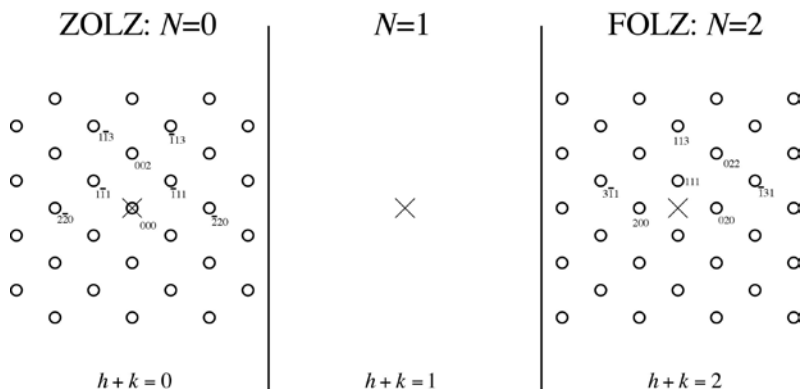
Next up is $N = 2$, with $\ell = 2$. By the same reasoning, this is the SOLZ.

ZAP indexing example: fcc [001]

This one should be easy, because we have already indexed sc [001], so we just need to erase the systematic absences. We find that 001 is no longer allowed for $N = 1$, but we still have 111 and 131, so $N = 1$ is still the FOLZ. The SOLZ has 002, with $N = 2$, so the assignment of the HOLZs as FOLZ, SOLZ, etc., doesn't change.

**ZAP indexing example: fcc [110]**

In this case, we have $h + k = N$. In addition to 000, the ZOLZ (which always has $N = 0$) contains 002 and $\bar{2}20$.

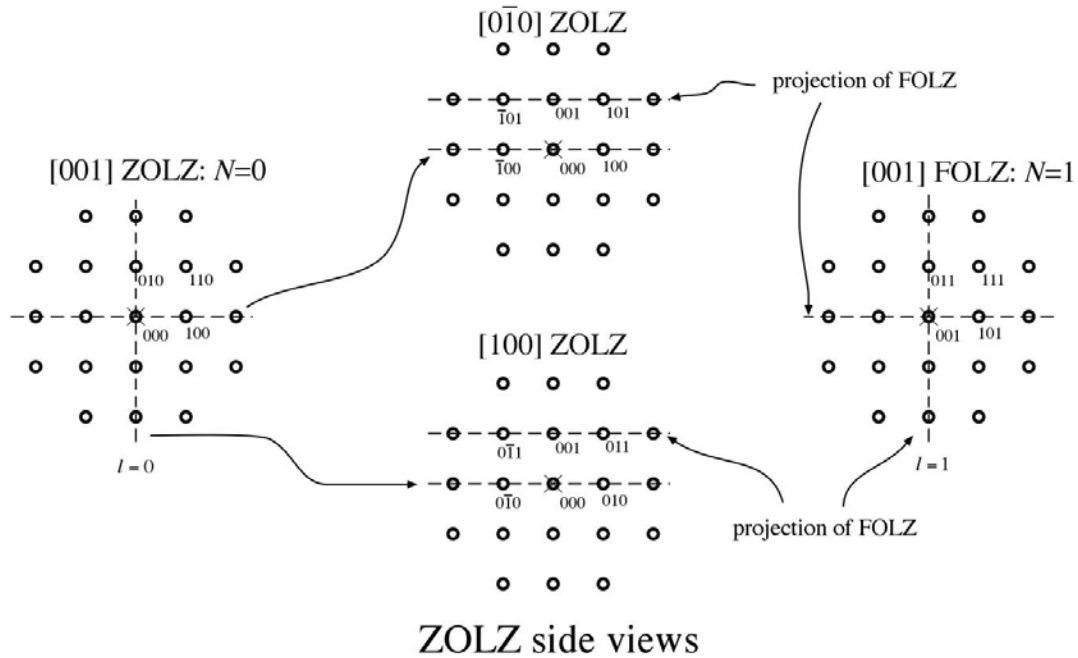


What about $N = 1$? Is it the FOLZ? We need to have $h + k = 1$, but if hkl are all even or all odd, there are no combinations of integers that satisfy this condition. So $N = 1$ is not a ZAP for fcc [110].

We then move on to $N = 2$. We can have $h + k = 2$, no problem, e.g., 020, 200. So $N = 2$ is a ZAP - It is the FOLZ!

Constructing HOLZ patterns example: sc [001]

Correctly drawing the ZAP for a HOLZ takes some thought. One can work back up the beam axis (out of the page) by imagining other ZOLZs that are perpendicular to the our zone axis of interest. Some of these will contain reflections that are also in our HOLZ ZAP. For example, if we want to find the [001] FOLZ, we can start with the [001] ZOLZ. The [100] ZOLZ is perpendicular to these, so it might contain some reflections in the [001] FOLZ. Those reflections reside in a systematic row of the [100] ZOLZ having $l = 1$ (e.g., 001, 011). Others can be found in the $[0\bar{1}0]$ ZOLZ (e.g., 101). Once we have the identities and locations of three reflections in the [001] FOLZ, we can navigate around to ID the rest.



Projecting onto the ZOLZ

We can decompose an RLV into components parallel and perpendicular to a HOLZ

$$\mathbf{g} = \mathbf{g}_{\parallel} + \mathbf{g}_{\perp}$$

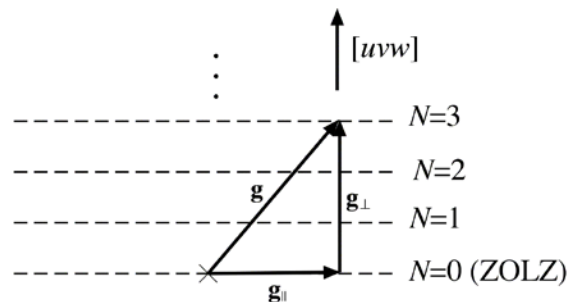
For reflections in the HOLZ, we now that $\mathbf{r}_{uvw} \cdot \mathbf{g} = N$. So $\mathbf{r}_{uvw} \cdot \mathbf{g}_{\perp} = N$ and $\mathbf{r}_{uvw} \cdot \mathbf{g}_{\parallel} = 0$. We could write

$$\mathbf{g}_{\perp} = N \cdot H \cdot \hat{\mathbf{r}}_{uvw} = N \cdot H \cdot \frac{\mathbf{r}_{uvw}}{|\mathbf{r}_{uvw}|}$$

Now take the dot product and use the zone law to find the Laue-zone separation H :

$$\mathbf{r}_{uvw} \cdot \mathbf{g}_{\perp} = N = N \cdot H \cdot |\mathbf{r}_{uvw}|, \text{ so } H = \frac{1}{|\mathbf{r}_{uvw}|}$$

Be aware, though, that some values of N may not correspond to Laue zones, so the actual separation could be an integer times H .



Cubic ZOLZ projection

Cubic has some nice properties we can use to simplify HOLZ indexing. For one thing, the direct- and reciprocal-lattice basis vectors are related by $\mathbf{b}_i = a^2 \cdot \mathbf{a}_i$. So the direct-lattice vector $\mathbf{r}_{uvw} = u\mathbf{a}_1 + v\mathbf{a}_2 + w\mathbf{a}_3$ that defines our zone axis is necessarily parallel to a RLV.

$$\mathbf{r}_{uvw} = a^2 \cdot (u\mathbf{b}_1 + v\mathbf{b}_2 + w\mathbf{b}_3)$$

Now we can find the Miller indices for the perpendicular component \mathbf{g}_\perp of an RLV in a particular HOLZ:

$$\mathbf{g}_\perp = \frac{N \cdot \mathbf{r}_{uvw}}{|\mathbf{r}_{uvw}|^2} = \frac{N \cdot \cancel{a^2} \cdot (u\mathbf{b}_1 + v\mathbf{b}_2 + w\mathbf{b}_3)}{\cancel{a^2} \cdot (u^2 + v^2 + w^2)} = h_\perp \mathbf{b}_1 + k_\perp \mathbf{b}_2 + \ell_\perp \mathbf{b}_3$$

We then now that the center of the HOLZ (aligned with 000) has Miller indices

$$(hkl)_\perp = \frac{N \cdot (uvw)}{u^2 + v^2 + w^2}$$

The in-plane components of the Miller indices are then

$$(hkl)_\parallel = (hkl) - (hkl)_\perp$$